ELECTRONIC APPLICATIONS OF NANOWIRES

CHAPTER 6: APPLICATIONS OF NANOWIRES IN LIGHT EMITTING DIODES

6.1. Introduction

Bottom-up nanowires are known for making semiconductor devices with high heterostructures due to strain relaxation by the nanowire sidewalls which permit the combination of highly lattice incompatible materials without forming dislocations. The resulting nanowires are utilized to fabricate LEDs (light-emitting diodes), solar cells, sensors, and lasers. However, costly single crystalline substrates are generally utilized as substrates for nanowire heterostructures also for epitaxial devices, which confines the manufacturability of nanowire devices (Sarwar et al., 2015; Zhao et al., 2015; 2016). Here, we determine nanowire LEDs grown directly and electrically incorporated on metal. Structural and optical measurements expose high-quality, vertically-aligned GaN nanowires on titanium and molybdenum films. Transmission electron microscopy endorses the composition disparity in the polarization-graded Al GaN nanowire light-emitting diodes. Blue to green electroluminescence is perceived from InGaN quantum well active areas, though GaN active regions show ultraviolet emission. These results determine a pathway for the huge-scale fabrication of solid-state lighting and optoelectronics on metal sheets or foils (Tchernycheva et al., 2014).

The III-Nitride semiconductor group has an extensive range of technologically significant applications, particularly in visible and ultraviolet LEDs (light-emitting diodes) and lasers (Taniyasu et al., 2006; Nakamura et al., 1994). High-class GaN thin films are usually grown on single crystalline sapphire substrates because of a good epitaxial relationship. Since the initial synthesis of GaN on sapphire major technological barriers have been overwhelmed to realize the commercialization of III-Nitride founded LEDs on sapphire like as comprehending p-type doping, mitigating electron overflow utilizing comprehensive bandgap AlGaN electron obstructive layer, and developing high-quality AlGaN and InGaN quantum wells (Maruska & Tietjen, 1969; Nakamura et al., 1992).

Lately, several research groups have been keenly working on III-N nanowires, and substantial progress has been stated on the growth mechanisms/method. Some normally used synthesis techniques comprise catalyst-founded nanowires, self-assembled catalyst open nanowires, and nanowires on selective area development or pre-patterned substrates. Materials synthesized utilizing catalysts undergo high concentrations of unwanted contaminations and specific area growth needs costly and complex processing steps. On the other hand catalyst, unrestricted GaN nanowires are free of these drawbacks (Gardner et al., 2007; Shatalov et al., 2012). Single crystalline Si substrates are generally utilized to produce self-assembled catalyst unrestricted GaN nanowires; Si has also the benefit of serving as a contact for optoelectronic and electronic devices. Though, one of the major

restrictive factors in the realization of huge-scale fabrication is the single-crystal Si substrate. It also confines performance as it engrosses light in optoelectronic devices. Gratefully, GaN nanowires have been revealed to grow on optically translucent amorphous SiO_x and glass substrates. These outcomes are proof that GaN nanowires don't require a universal epitaxial relationship with the substrate and could be grown on largely accessible substrates (Calarco et al., 2007; Ristić et al., 2008).

6.2. LED growth Mechanisms

Here we report the direct development and electrical incorporation of III-Nitride nanowire LEDs on metal. Initially, the growth of GaN nanowires on tinny Ti and Mo films on Si wafers is revealed. PL (Photoluminescence) measurements present the same optical quality for the nanowires grown on Si wafers related to those grown on metal. Room temperature band edge PL release at 363 nm with a 10 nm FWHM (full width at half maximum) is perceived however below bandgap fault-related PL is missing. Further, nanowire LEDs comprised of polarization graded AlGaN nanowires on tinny Mo films are fabricated with a diversity of GaN and InGaN active regions (McCune et al., 2012; Li et al., 2015). The EL (electroluminescence) from InGaN nanowire LEDs is diverse from blue to green (450 to 565 nm) with the highest efficiency at 230 A/cm^2 and 3 percent efficiency fall at 500 A/cm^2. Modeling of the EQE (external quantum efficiency) utilizing the ABC model discloses a maximum IQE (internal quantum efficiency) of ~47% which is similar to the stated typical IQE values for visible GaN founded nanowire LEDs on Si. Lastly, nanowire LEDs developed on Mo films comprising GaN active regions release at ultraviolet (385nm) wavelengths. The selection of Mo metal film is overseen by the fact that our nanowire LEDs present a p-down orientation because of the utilization of polarization-induced doping and Mo is predicted to make good electrical interaction with p-type GaN because of its comparatively large work function. Moreover, it is a safe material for MBE (molecular beam epitaxy) environment because of its high low vapor pressure at high temperatures (Zimmler et al., 2009; Kent et al., 2014).

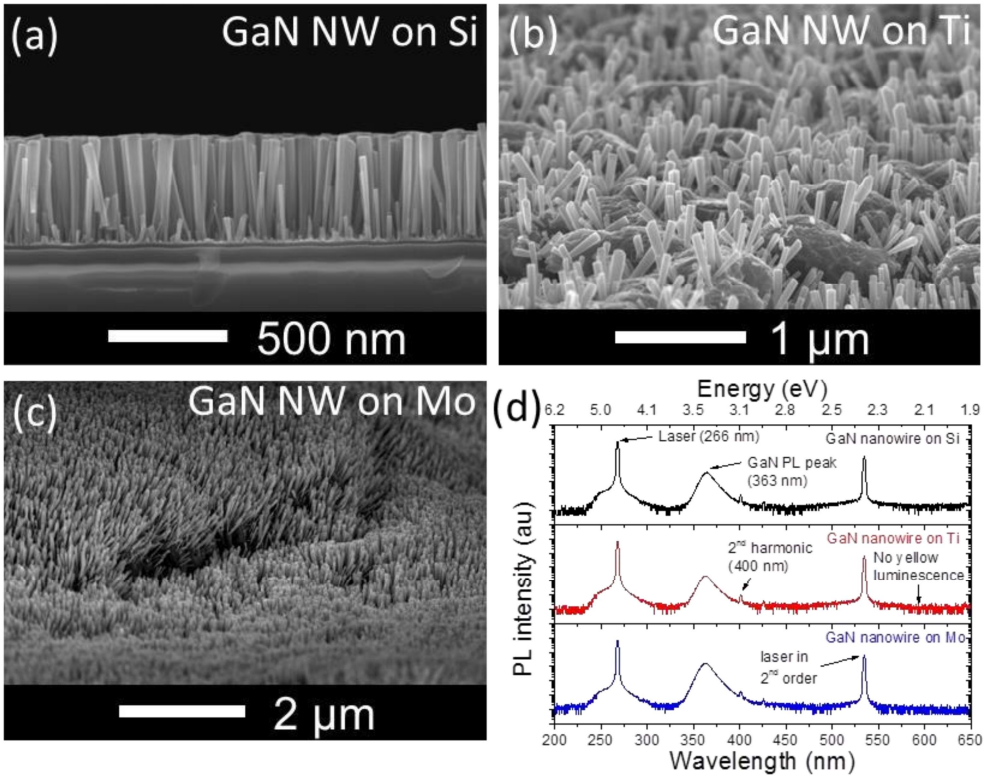

Figure 6.1. Developing semiconductor nanowires on metal films. SEM (Scanning electron microscopy) images of GaN nanowires developed on (a) Si, (b) Ti, and (c) Mo. (d) Room temperature PL (photoluminescence) measurements of GaN nanowires developed on Si (black line), Ti (red line), and Mo (blue line).

[https://onlinelibrary.wiley.com/doi/abs/10.1002/smll.201501909]

Self-assembled catalyst unrestricted GaN nanowires are developed directly on Mo and Ti films utilizing PAMBE (plasma-assisted molecular beam epitaxy). To confirm identical growth situations, one-quarter of the wafer is covered with Mo, another quarter is covered with Ti and the remaining wafer is left as bare Si. The metal-covered Si wafer is moved to the MBE growth section and native oxide desorption is executed *in-situ* through heating the substrate to 1000° C for 1 minute with a ramp rate of 50° C/min underneath a vacuum of ~7×10^{-11} torr. Figure 1(a), (b), and (c) display the SEM (scanning electron microscopy) images of the nanowires developed on Si, Ti, and Mo, respectively. As predicted, the nanowires on Si show vertical orientation. Statistical examination of the SEM images tells that diameter and density of the nanowires on Si are 34.75±8.56 nm and 209±12 μm^{-2}, respectively (Guo et al., 2010; Rigutti et al., 2010). It is found that nanowires developed on Ti film show comparatively lower density and larger diameter (54.77±7.76 nm) however nanowires developed on Mo film display the same density and diameter (35.75±5.81 nm) related to the nanowires developed on Si. In both metals, delamination of the film from the Si wafer is perceived, as shown in Figure 6. 1 (b) and (c). We speculate that this happens because of the large thermal growth

mismatch among Si (2.6-3.3×10^{-6} K^{-1}) and metal films (Ti: 8.4-8.6×10^{-6} K^{-1} and Mo: 4.8-5.1×10^{-6} K^{-1}). Furthermore, the high temperature (1000° C) *in-situ* oxide desorption phase could also contribute to the delamination of metal films. Utilizing of small ramp rate and missing the *in-situ* oxide desorption phase (which is not compulsory if exclusively grown on metal) is found to assist decrease the delamination problem and utilized for later samples (Bertness et al., 2010; Ra et al., 2014).

Figure 1 (d) displays the room temperature PL (photoluminescence) release spectra from nanowires developed on Ti (red), Mo (blue), and Si (black). Nanowires developed on all 3 substrates display only a single PL peak release at 363 nm (~3.423 eV) with FWHM of 10 nm, which links to the band to band carrier recombination in GaN. Further, sub-bandgap features are not perceived over the measured spectral extent (300 to 650 nm). PAMBE developed GaN nanowires on Si are stated to be closely dislocation-free and don't show defect-mediated yellow luminescence which is very usual in GaN thin films. The lack of yellow luminesce from nanowires developed on Mo or Ti films shows that nanowires developed on metal films have similar quality as nanowires developed on single crystalline Si wafers (Glas, 2006; Wang et al., 2015).

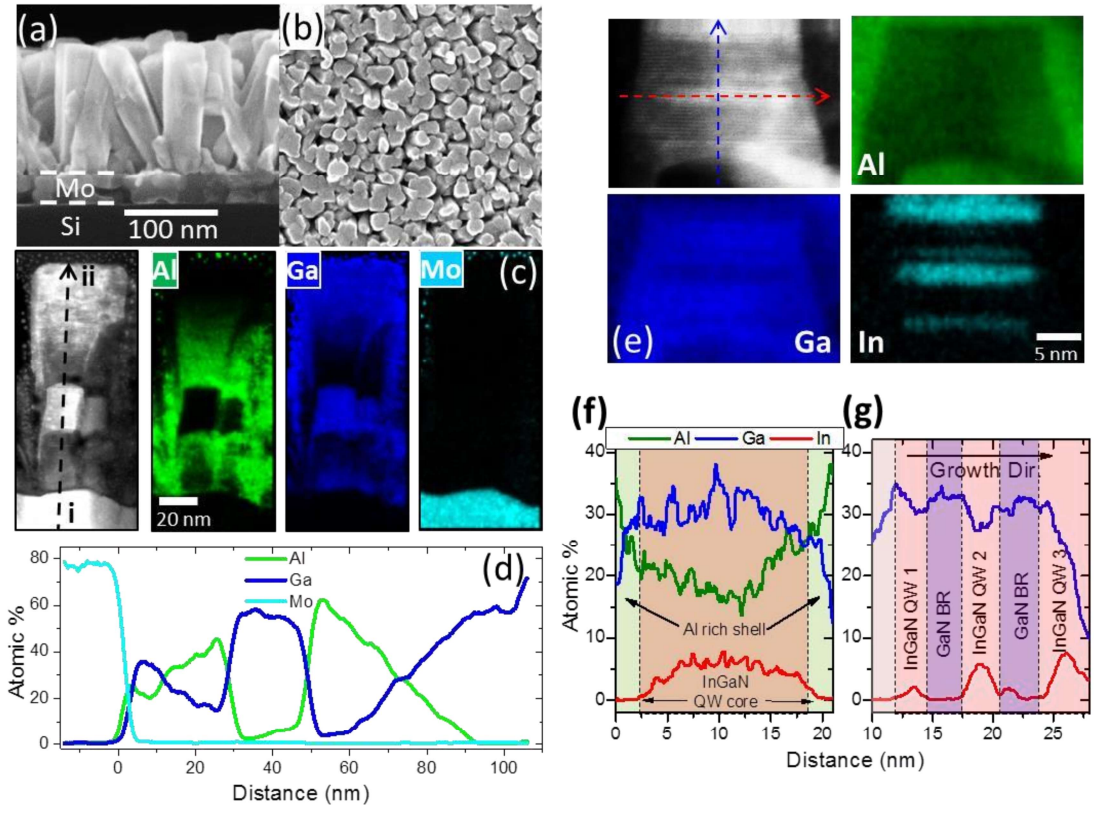

Figure 6.2. Chemical mapping of the compositional fluctuation in nanowire heterostructures developed on metal.

[https://onlinelibrary.wiley.com/doi/10.1002/smll.201501909

Note:

(a) Cross-section and (b) plan vision SEM images of classified AlGaN nanowire LEDs developed on Mo films placed on Si substrate. (c) HAADF (High angle annular dark field) STEM (scanning transmission electron microscopy) image along with EDXS (energy dispersive x-ray spectroscopy) chemical composition maps displaying back and forth composition grouping. (d) EDXS line scan together with the axis (i-ii in Figure 6. 2(c)) of the nanowire heterostructure displaying approximately linear difference of Ga and Al composition. Mo signal could be observed from underneath the nanowire. (e) HAADF STEM image of the active area of a single nanowire. Al, In and Ga composition maps are also shown. (f) EDXS line scan besides the radial direction by the 2nd QW (quantum well) showing InGaN QW enfolded in an Al-rich AlGaN shell. (g) EDXS line scan alongside the axis of the active area showing 3 InGaN QWs with enhancing in composition in the growth direction.

After effectively developing high-quality GaN nanowires on the metal films, we grow and describe nanowire LEDs on metal with together visible and near UV (ultraviolet) emitting active areas. The design of the nanowire LED heterostructure takes benefit of the intrinsic polarization of III-Nitride materials. When compositionally classified, the polarization forms 3D distributed bound charge. At this point, we nucleate Mg-doped GaN nanowires on Mo films utilizing PAMBE at 720° C. An earlier study exhibited that catalyst-free PAMBE developed GaN nanowires grow especially in the $(000\bar{1})$ crystallographic direction (N-face) (Meijers et al., 2006; Consonni et al., 2010). Following nucleation, the configuration of the nanowire is linearly classified using a shutter pulsing technique from GaN to AlN over 50 nm. This forms a 6.5×10^{18} cm^{-3} negative bound polarization charge, causing p-type conductivity. A dynamic region is comprised of 3× InGaN/GaN quantum wells put at 625° C. Further, a 100 nm AlN to GaN linearly graded layer is placed to persuade polarization doped n-type layer. The top (n-type) and bottom (p-type) graded areas are doped with Si and Mg, respectively. Attentive readers are directed to ref. (Golam Sarwar et al., 2015) for details on polarization-induced doping in the classified AlGaN nanowires and their confines (Park et al., 2005; Songmuang et al., 2007).

Figure 6. 2 (a) and (b) display the cross-section and plan-view SEM pictures of the nanowire LED heterostructure, correspondingly. Closely vertically aligned high-density nanowires are perceived on the Mo film. Figure 6. 2(c) displays HAADF (high angle annular dark field) STEM (scanning transmission electron microscopy) image and EDXS (energy dispersive x-ray spectroscopy) chemical composition (Ga, Mo, and Al) maps in the nanowire heterostructure. Chemical composition diagrams show an extreme Ga concentration at the top and base of the nanowire and the highest Al concentration at the center of the nanowire endorsing the back and forth compositional classifying in

the vertical direction (Debnath et al., 2007; Tchernycheva et al., 2007). Displayed in Figure 6. 2(d), the EDXS line scan alongside the growth direction (i-ii in Figure 6. 2(c)) exhibits the desired linear alteration in Al and Ga composition in the p and n- side as designed. The Ga rich portion at the mid of the nanowire (Figure 6. 2(c)) links to the active region. We don't see an obvious In signal from the active area, which is likely because of the overlapping of numerous nanowires in this sample made utilizing FIB. Though, In signal is perceived from a single nanowire that is discrete on a TEM grid. Figure 6. 2(e) displays a HAADF STEM image of the active area of a nanowire LED and related chemical composition diagrams (In, Al and Ga). An EDXS line scan alongside the radial direction (red line in Figure 6. 2(e)) by an InGaN quantum well (Figure 6. 2(f)) displays a defined InGaN core region covered with an Al-rich AlGaN shell. The impulsive creation of an Al-rich AlGaN shell region is the consequence of the low adatom mobility of Al linked to Ga and In at high temperatures. The Al adatoms intruding on the side walls integrate where they land earlier they could diffuse to the top of the nanowire (Bertness et al., 2010). On the other hand, Ga and In adatoms have greater mobility (compared to Al) and could diffuse towards the uppermost of the nanowire and integrate there. A line-scan alongside the axis of the active area (blue line in Figure 6. 2(e)) displays the formation of 3 InGaN quantum wells detached by GaN barriers, revealed in Figure 6. 2(g). The In composition and width of the quantum wells are found to enhance in subsequent quantum wells. This kind of variation in composition and width is observed earlier in InGaN/GaN nanowire heterostructure through Tourbot et al. (2012). The authors accredited this fluctuation to the composition pulling effect. It is worth noticing that the EDXS analysis is executed without a standard and because of the complicated core-shell geometry of the nanowires the composition attained in this analysis is not entire.

Nanowire LED devices are made-up through depositing a 5 nm Ti / 10 nm Au semitransparent top contact right onto the uppermost of the nanowires. A 300 nm Au grid is placed on top of the semitransparent contact as a current dispersion layer. In-diffused bottom contact is created on the Si substrate after mechanically eliminating the nanowires (Hsiao et al., 2006).

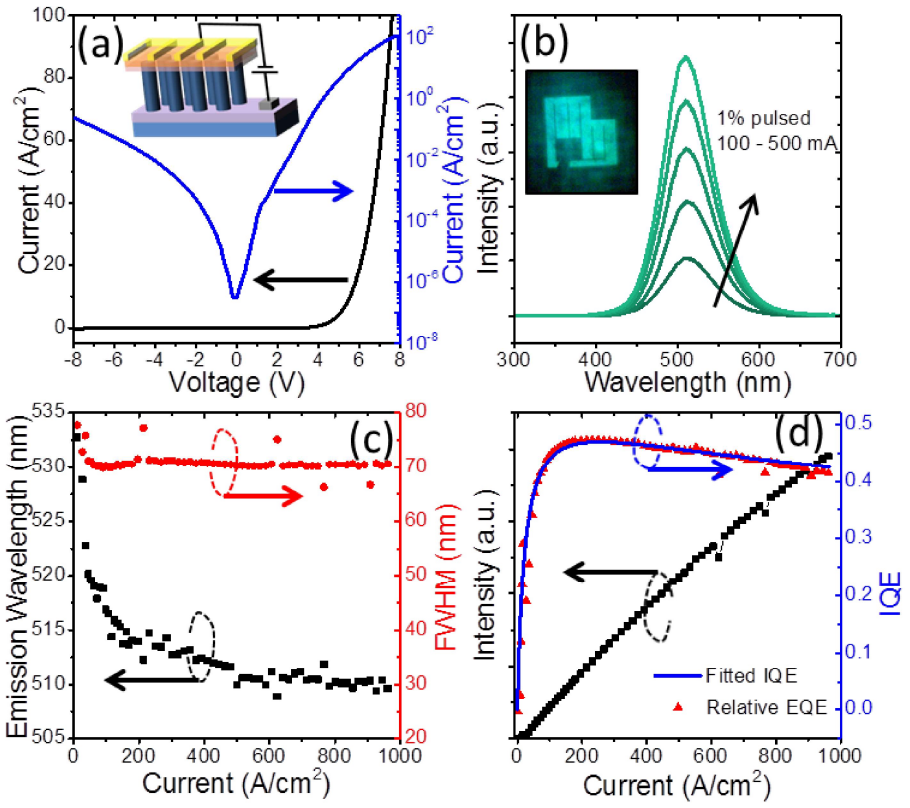

Figure 6.3. Green nanowire LEDs developed on metal with InGaN quantum well active areas.

[https://www.researchgate.net/figure/Characteristics-of-AlGaN-nanowire-LEDs-The-p-metal-size-is-500-m-500-m-a_fig4_307443890]

Note:

(a) Current-voltage characteristic of nanowire LED on the Mo film. Insertion displays the schematic of the contact creation scheme. (b) EL (Electroluminescence) spectra under pulsated current excitation of an InGaN QW nanowire LED developed on Mo film releasing near the green band. Inset displays an optical picture of an LED device in operation. (c) Highest discharge wavelength (black squares) FWHM (full width at half maximum) as a function of current density. (d) EL highest intensity (black squares) and comparative EQE (red triangles) as a function of injection current density. IQE (blue line) is modeled through fitting relative EQE utilizing the ABC model.

The diagram of the contact creation scheme is displayed in the inset of Figure 6. 3(a). A DC current-voltage (I-V) characteristic of a nanowire LED device is displayed in Figure 6. 3(a). Diode conduct having a threshold voltage of ~6V is perceived. EL measurements are executed on 300×300 μm^2 LED devices under pulsed (~1 percent duty cycle) current excitation to reduce any junction heating effect. Figure 6. 3(b) displays EL spectra from a device below excitation over the range of 100 – 500 mA in 100 mA steps. The insertion of Figure 6. 3(b) displays an optical image of the nanowire LED

device functioning under DC excitation. A video of functioning nanowire LED on Mo film could be found in the additional information (Bertness et al., 2006). The highest emission at ~510 nm is witnessed which corresponds to discharge from the numerous InGaN quantum wells. Figure 6. 3(c) displays the highest emission wavelength (black squares) and FWHM (full width at half maximum) (red circles) as a purpose of injection current density. The highest emission moves from ~532 nm (at low injection) to ~510 nm (at high injection). We aspect this blue move to a combination of 2 factors. First, this could be due to the quantum restricted Stark effect in individual QWs usually observed in nitride-founded polar quantum wells. Second, this could be the outcome of a slight fluctuation in In composition in QWs. Because of better electron injection related to hole injection, discharge from the third QW (near to n-side graded region) leads to low injection. With the rise in carrier injection, discharge from second and first QW causes the blue move due to reduced In composition (i.e. high bandgap) in these QWs. The FWHM reduces from 77.7 nm at low injection to 70.6 nm at high injection. Figure 6. 3(d) displays the highest emission intensity (black squares) and relative EQE (external quantum efficiency) (red triangles) as a function of current density. The highest emission intensity rises linearly from low to moderate injection and displays alteration from linearity at high current density. EQE displays a rise with current density and highest at ~230 A/cm^2. EQE value falls by 3 percent at 500 A/cm^2 and 12 percent at 1000 A/cm^2, compared to the peak EQE value (Carnevale et al., 2011).

The IQE of an LED could be modeled utilizing the ABC model.

$$IQE = \frac{Bn^2}{An + Bn^2 + Cn^3}$$

Here, A is the Shockley-Read-Hall non-radiative recombination coefficient, B is the radiative recombination coefficient, C signifies higher-order carrier loss because of Auger recombination and/or carrier runoff, and n is the carrier concentration in the active area. EQE is the product of EE (Extraction Efficiency) and IQE. Supposing EE to be free of injection current density, IQE is modeled by fitting the shape of EQE utilizing the ABC model. Using this technique we found A, B and C are 2×10^8 s^{-1}, 2.5×10^{-10} cm^{3}s^{-1}, and 10^{-28} cm^{6}s^{-1}, correspondingly, for our nanowire devices, very near to the stated values for InGaN nanowire LEDs. The extreme IQE is found to be ~ 47 percent which lies in the reported value range (40-50 percent) for obvious nanowire LEDs (Hersee et al., 2006).

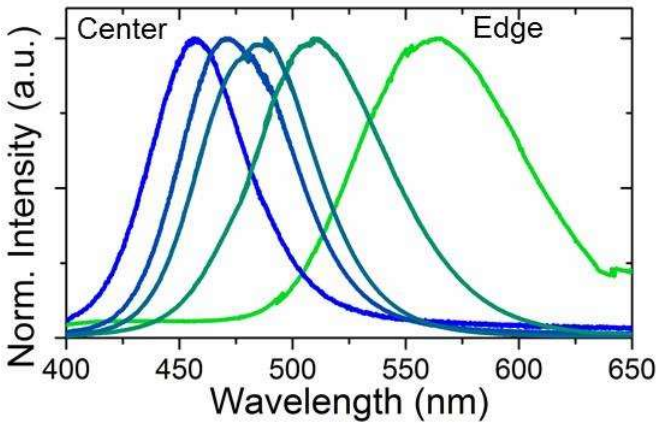

Figure 6.4. Display of blue to green nanowire LEDs developed on metal. An extensive range of emission wavelengths is witnessed from different areas of a 3-inch wafer covered with Mo because of the temperature sensitivity of In integration in the InGaN active regions

[https://www.led-professional.com/resources-1/articles/full-color-ingan-algan-nanowire-light-emitting-diodes-for-ssl-and-displays]

The nanowires in this study are developed on a 3-inch wafer. Figure 6. 4 displays emission spectra of the LED devices measured from diverse locations of the wafer. Right-most (leftmost) signifies an LED device from the center (edge) of the wafer. We noticed an alteration in the emission wavelength from LED devices through the wafer. We aspect this fluctuation to the temperature incline across the three-inch substrate throughout nanowire deposition (Stoica et al., 2008). It is well-identified that InGaN composition is a durable function of temperature which outcomes in higher In incorporation in the QWs at the edge (low temperature) than in the middle (high temperature) region. Moreover, SEM images examine on the nanowire samples shown smaller average diameters (31.6 nm) at the midpoint (high temperature) of the wafer compared to the average diameter (39.9 nm) at the border (low temperature) of the wafer. R. Armitage et al. have shown that In integration in nanowires enhancing with increasing diameter. These two facts describe the blue shift witnessed in the EL spectra in Figure 6. 4 from the edge to midpoint region (Duan & Lieber, 2000).

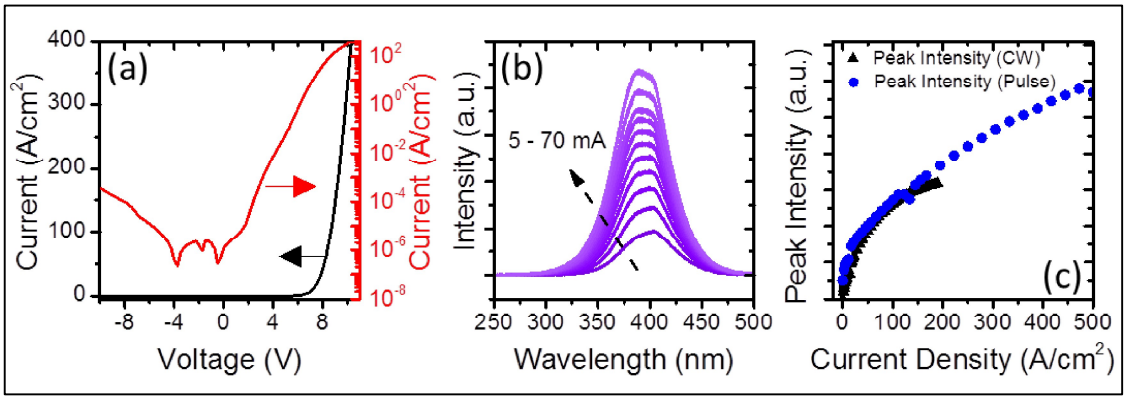

Figure 6.5. Ultraviolet nanowire LEDs developed on metal.

[https://onlinelibrary.wiley.com/doi/abs/10.1002/smll.201501909]

Note:

(a) Current-voltage characteristic of a GaN QW nanowire LED developed on Mo film. (b) EL (Electroluminescence) spectra underneath pulsed current excitation of a GaN QW nanowire LED developed on Mo film releasing near-ultraviolet wavelength. (c) EL highest intensity under the constant wave, pulsed (blue circles) and CW (black triangles) current as a purpose of injection current density.

6.3. PAMBE growth of GaN Nanowires

Self-assembled catalyst unrestricted GaN nanowires are developed using Veeco Gen 930 PAMBE (plasma-assisted molecular beam epitaxy) system. Ti and Mo thin films (~50 nm) are deposited utilizing electron beam evaporation on a 3 inch Si (111) wafer. Nanowires are grown utilizing the two-step dynamic growth process described in Carnevale et al. (2011). In this technique, nanowires are nucleated at a low temperature until necessary nanowire density is attained followed by a high-temperature growth in which previously nucleated nanowires carry on to grow however new nanowire nucleation doesn't happen. GaN nanowires are nucleated at 720° C for 5 min and developed at 790° C for 2 hours. A nitrogen partial pressure of 2×10^{-5} torr is utilized having a plasma power of 350W (Kuykendall et al., 2014).

6.4. Structural Characterization

SEM images are collected utilizing an FEI/Philips Sirion SEM with a FE (field emission) source and an in-lens secondary electron detector. STEM samples are made with a Helios NanoLab 600 dual-beam FIB (focused ion beam). High-resolution STEM imaging is worked out on an FEI image

modified Titan^{3TM} G2 60-300 S/TEM furnished with a quad silicon drift detector at 300 kV (Schuster et al., 2015).

6.5. Photoluminescence

The nanowires are optically eager utilizing the third harmonic (266 nm) of a mode-locked Ti: sapphire oscillator (Coherent Chameleon Ultra II) functioning at 800 nm and 40 MHz. The samples are brightened with an average power of 0.5 mW and attentive on the sample surface by a 0.5 NA 36× reflective objective which consequences in a beam diameter of ~10 μm. The discharge from the samples is gathered through a 300 nm long-pass filter and agreed to a 0.5 m spectrometer (Princeton Instruments SP2500i) armed with a UV–vis CCD (Princeton Instruments PIXIS100) and a 1200 g/mm diffraction grating (Gačević et al., 2015).

References

Bertness, K. A., Roshko, A., Sanford, N. A., Barker, J. M., & Davydov, A. V. (2006). Spontaneously grown GaN and AlGaN nanowires. *Journal of Crystal Growth*, *287*(2), 522-527.

Bertness, K. A., Sanford, N. A., & Davydov, A. V. (2010). GaN nanowires grown by molecular beam epitaxy. *IEEE Journal of selected topics in quantum electronics*, *17*(4), 847-858.

Bertness, K. A., Sanford, N. A., & Davydov, A. V. (2010). GaN nanowires grown by molecular beam epitaxy. *IEEE Journal of selected topics in quantum electronics*, *17*(4), 847-858.

Calarco, R., Meijers, R. J., Debnath, R. K., Stoica, T., Sutter, E., & Lüth, H. (2007). Nucleation and growth of GaN nanowires on Si (111) performed by molecular beam epitaxy. *Nano letters*, *7*(8), 2248-2251.

Carnevale, S. D., Yang, J., Phillips, P. J., Mills, M. J., & Myers, R. C. (2011). Three-dimensional GaN/AlN nanowire heterostructures by separating nucleation and growth processes. *Nano letters*, *11*(2), 866-871.

Consonni, V., Knelangen, M., Geelhaar, L., Trampert, A., & Riechert, H. (2010). Nucleation mechanisms of epitaxial GaN nanowires: Origin of their self-induced formation and initial radius. *Physical Review B*, *81*(8), 085310.

De Cremoux, B. (1982). INSTABILITY CRITERIA IN TERNARY AND QUATERNARY II IV EPITAXIAL SOLID SOLUTIONS. *Le Journal de Physique Colloques* , *43* (C5), C5-19.

Debnath, R. K., Meijers, R., Richter, T., Stoica, T., Calarco, R., & Lüth, H. (2007). Mechanism of molecular beam epitaxy growth of GaN nanowires on Si (111). *Applied Physics Letters*, *90*(12), 123117.

Duan, X., & Lieber, C. M. (2000). Laser-assisted catalytic growth of single crystal GaN nanowires. *Journal of the American Chemical Society*, *122*(1), 188-189.

Gačević, Z., Gomez Sanchez, D., & Calleja, E. (2015). Formation mechanisms of GaN nanowires grown by selective area growth homoepitaxy. *Nano letters*, *15*(2), 1117-1121.

Gardner, N. F., Müller, G. O., Shen, Y. C., Chen, G., Watanabe, S., Götz, W., & Krames, M. R. (2007). Blue-emitting InGaN–GaN double-heterostructure light-emitting diodes reaching maximum quantum efficiency above 200 A⁄ cm 2. *Applied Physics Letters*, *91*(24), 243506.

Glas, F. (2006). Critical dimensions for the plastic relaxation of strained axial heterostructures in free-standing nanowires. *Physical Review B*, *74*(12), 121302.

Golam Sarwar, A. T. M., Carnevale, S. D., Kent, T. F., Yang, F., McComb, D. W., & Myers, R. C. (2015). Tuning the polarization-induced free hole density in nanowires graded from GaN to AlN. *Applied Physics Letters*, *106*(3), 032102.

Guo, W., Zhang, M., Banerjee, A., & Bhattacharya, P. (2010). Catalyst-free InGaN/GaN nanowire light emitting diodes grown on (001) silicon by molecular beam epitaxy. *Nano letters*, *10*(9), 3355-3359.

Hersee, S. D., Sun, X., & Wang, X. (2006). The controlled growth of GaN nanowires. *Nano letters*, *6*(8), 1808-1811.

Hsiao, C. L., Tu, L. W., Chi, T. W., Seo, H. W., Chen, Q. Y., & Chu, W. K. (2006). Buffer controlled GaN nanorods growth on Si (111) substrates by plasma-assisted molecular beam epitaxy. *Journal of Vacuum Science & Technology B: Microelectronics and Nanometer Structures Processing, Measurement, and Phenomena*, *24*(2), 845-851.

Kent, T. F., Carnevale, S. D., Sarwar, A. T. M., Phillips, P. J., Klie, R. F., & Myers, R. C. (2014). Deep ultraviolet emitting polarization induced nanowire light emitting diodes with AlxGa1− xN active regions. *Nanotechnology*, *25*(45), 455201.

Kuykendall, T. R., Altoe, M. V. P., Ogletree, D. F., & Aloni, S. (2014). Catalyst-directed crystallographic orientation control of GaN nanowire growth. *Nano letters*, *14*(12), 6767-6773.

Li, K. H., Liu, X., Wang, Q., Zhao, S., & Mi, Z. (2015). Ultralow-threshold electrically injected AlGaN nanowire ultraviolet lasers on Si operating at low temperature. *Nature nanotechnology*, *10*(2), 140.

Maruska, H. P., & Tietjen, J. J. (1969). The preparation and properties of vapor-deposited single-crystal-line GaN. *Applied Physics Letters*, *15*(10), 327-329.

McCune, M., Zhang, W., & Deng, Y. (2012). High efficiency dye-sensitized solar cells based on three-dimensional multilayered ZnO nanowire arrays with "caterpillar-like" structure. *Nano letters*, *12*(7), 3656-3662.

Meijers, R., Richter, T., Calarco, R., Stoica, T., Bochem, H. P., Marso, M., & Lüth, H. (2006). GaN-nanowhiskers: MBE-growth conditions and optical properties. *Journal of crystal growth*, *289*(1), 381-386.

Nakamura, S., Iwasa, N., Senoh, M., & Mukai, T. (1992). Hole compensation mechanism of p-type GaN films. *Japanese Journal of Applied Physics*, *31*(5R), 1258.

Nakamura, S., Mukai, T., & Senoh, M. (1994). Candela-class high-brightness InGaN/AlGaN double-heterostructure blue-light-emitting diodes. *Applied Physics Letters*, *64*(13), 1687-1689.

Park, Y. S., Lee, S. H., Oh, J. E., Park, C. M., & Kang, T. W. (2005). Self-assembled GaN nano-rods grown directly on (1 1 1) Si substrates: Dependence on growth conditions. *Journal of crystal growth*, *282*(3-4), 313-319.

Ra, Y. H., Navamathavan, R., Yoo, H. I., & Lee, C. R. (2014). Single nanowire light-emitting diodes using uniaxial and coaxial InGaN/GaN multiple quantum wells synthesized by metalorganic chemical vapor deposition. *Nano letters*, *14*(3), 1537-1545.

Rigutti, L., Tchernycheva, M., De Luna Bugallo, A., Jacopin, G., Julien, F. H., Zagonel, L. F., ... & Songmuang, R. (2010). Ultraviolet photodetector based on GaN/AlN quantum disks in a single nanowire. *Nano letters*, *10*(8), 2939-2943.

Ristić, J., Calleja, E., Fernández-Garrido, S., Cerutti, L., Trampert, A., Jahn, U., & Ploog, K. H. (2008). On the mechanisms of spontaneous growth of III-nitride nanocolumns by plasma-assisted molecular beam epitaxy. *Journal of crystal growth*, *310*(18), 4035-4045.

Sarwar, A. G., Carnevale, S. D., Yang, F., Kent, T. F., Jamison, J. J., McComb, D. W., & Myers, R. C. (2015). Semiconductor nanowire light-emitting diodes grown on metal: a direction toward large-scale fabrication of nanowire devices. *Small*, *11*(40), 5402-5408.

Schuster, F., Hetzl, M., Weiszer, S., Garrido, J. A., De La Mata, M., Magen, C., ... & Stutzmann, M. (2015). Position-controlled growth of GaN nanowires and nanotubes on diamond by molecular beam epitaxy. *Nano letters*, *15*(3), 1773-1779.

Shatalov, M., Sun, W., Lunev, A., Hu, X., Dobrinsky, A., Bilenko, Y., ... & Wraback, M. (2012). AlGaN deep-ultraviolet light-emitting diodes with external quantum efficiency above 10%. *Applied Physics Express*, *5*(8), 082101.

Songmuang, R., Landré, O., & Daudin, B. (2007). From nucleation to growth of catalyst-free GaN nanowires on thin AlN buffer layer. *Applied Physics Letters*, *91*(25), 251902.

Stoica, T., Sutter, E., Meijers, R. J., Debnath, R. K., Calarco, R., Lüth, H., & Grützmacher, D. (2008). Interface and wetting layer effect on the catalyst-free nucleation and growth of GaN nanowires. *Small*, *4*(6), 751-754.

Taniyasu, Y., Kasu, M., & Makimoto, T. (2006). An aluminium nitride light-emitting diode with a wavelength of 210 nanometres. *nature*, *441*(7091), 325-328.

Tchernycheva, M., Lavenus, P., Zhang, H., Babichev, A. V., Jacopin, G., Shahmohammadi, M., ... & Kryliouk, O. (2014). InGaN/GaN core–shell single nanowire light emitting diodes with graphene-based p-contact. *Nano letters*, *14*(5), 2456-2465.

Tchernycheva, M., Sartel, C., Cirlin, G., Travers, L., Patriarche, G., Harmand, J. C., ... & Julien, F. (2007). Growth of GaN free-standing nanowires by plasma-assisted molecular beam epitaxy: structural and optical characterization. *Nanotechnology*, *18*(38), 385306.

Tourbot, G., Bougerol, C., Glas, F., Zagonel, L. F., Mahfoud, Z., Meuret, S., ... & Daudin, B. (2012). Growth mechanism and properties of InGaN insertions in GaN nanowires. *Nanotechnology*, *23*(13), 135703.

Wang, R., Liu, X., Shih, I., & Mi, Z. (2015). High efficiency, full-color AlInGaN quaternary nanowire light emitting diodes with spontaneous core-shell structures on Si. *Applied Physics Letters*, *106*(26), 261104.

Zhao, C., Ng, T. K., ElAfandy, R. T., Prabaswara, A., Consiglio, G. B., Ajia, I. A., ... & Ooi, B. S. (2016). Droop-free, reliable, and high-power InGaN/GaN nanowire light-emitting diodes for monolithic metal-optoelectronics. *Nano letters*, *16*(7), 4616-4623.

Zhao, S., Connie, A. T., Dastjerdi, M. H. T., Kong, X. H., Wang, Q., Djavid, M., ... & Mi, Z. (2015). Aluminum nitride nanowire light emitting diodes: Breaking the fundamental bottleneck of deep ultraviolet light sources. *Scientific reports*, *5*(1), 1-5.

Zimmler, M. A., Voss, T., Ronning, C., & Capasso, F. (2009). Exciton-related electroluminescence from ZnO nanowire light-emitting diodes. *Applied Physics Letters*, *94*(24), 241120.